Conference paper

Zahid Shafiq, Muhammad Ajmal*, Sonia Kiran, Sonia Zulfiqar, Ghazala Yasmeen, Muzaffar Iqbal, Zahoor H. Farooqi, Zaheer Ahmad, Nurettin Sahiner, Khalid Mahmood, Hafiz Badaruddin Ahmad and Ahmed Al-Harrasi

Facile synthesis of hydrogel-nickel nanoparticle composites and their applications in adsorption and catalysis

https://doi.org/10.1515/pac-2018-1201

Abstract: Homopolymer bulk hydrogel of methacrylic acid was synthesized through a new single-step facile rout and used as a template for the fabrication of nickel (Ni) nanoparticles and as adsorbent to remove methylene blue (MB) and Rhodamine-6G (Rh-6G) from water. The Ni nanoparticles containing composite hydrogel was applied as catalyst for the degradation of a nitro compound. The carboxylic groups acted as highly efficient adsorption sites and their high degree was responsible for the removal of huge amounts of MB and Rh-6G from water. The maximum adsorption capacity of poly (methacrylic acid) hydrogel was 685 mg g^{-1} for MB and 1571 mg g^{-1} for Rh-6G. The adsorption data of MB was best fitted with Langmuir adsorption isotherm while that of Rh-6G with Temkin adsorption isotherm. Catalytic property of prepared hydrogel integrated with Ni nanoparticles was evaluated by using it as a catalyst for the degradation of 4-nitrophenol (4-NP). The apparent rate constant (k_{app}) observed in this study for the reduction of 4-NP was as high as 0.038 min^{-1}. It was found that this catalyst system can be used repetitively with a slight decrease in catalytic activity.

Keywords: adsorption; catalysis; Eurasia 2018; hydrogel; nanoparticles; waste water.

Introduction

Hydrogels have become appealing materials for waste water treatment [1]. Depending upon chemical composition, hydrogels may have potential to decontaminate water in terms of removing the organic and inorganic pollutants by adsorption; a method considered as the most appropriate one for the elimination

Article note: A collection of invited papers based on presentations at the 15th Eurasia Conference on Chemical Sciences ($EuAsC_2S$-15) held at Sapienza University of Rome, Italy, 5–8 September 2018.

***Corresponding author: Muhammad Ajmal,** Department of Chemistry, University of Education, Attock Campus, Attock 43600, Pakistan, Tel.: +92 3085513305, E-mail: m.ajmal65@yahoo.com
Zahid Shafiq, Sonia Kiran, Sonia Zulfiqar, Ghazala Yasmeen, Khalid Mahmood and Hafiz Badaruddin Ahmad: Institute of Chemical Sciences, Bahauddin Zakariya University, Multan 60800, Pakistan
Muzaffar Iqbal: National Centre for Nanoscience and Technology, University of Chinese Academy of Sciences, Beijing 100190, China
Zahoor H. Farooqi: Institute of Chemistry, University of the Punjab, New Campus, Lahore 54590, Pakistan
Zaheer Ahmad: Department of Chemistry, University of Wah, Quaid Avenue, Wah Cantt. 47040, Pakistan
Nurettin Sahiner: Canakkale Onsekiz Mart University, Faculty of Science and Arts, Chemistry Department, Terzioglu Campus, 17100 Canakkale, Turkey
Ahmed Al-Harrasi: UoN Chair of Oman's Medicinal Plants and Marine Natural Products, University of Nizwa, P.O. Box 33, Birkat Al Mauz, Nizwa 616, Sultanate of Oman

of many types of toxins from wastewaters [2]. Hydrogels can be engineered by fabricating with a variety of nanomaterials which can be helpful for the catalytic degradation of water pollutants [3]. Architecting of hydrogels with various functional groups including –COOH,–SO_3H, –SH,–OH, and –NH_2 enables them to adsorb high amounts of positively and negatively charged pollutants such as cationic and anionic dyes, heavy metal ions, herbicides, pesticides, insecticides etc. which may be contaminated in water from different industries [4]. The remarkable swelling ability of hydrogels offers an easy and hence rapid entrance of adsorbate into the hydrogel networks while their insolubility makes it easy to remove these adsorbents from water after completion of adsorption task. These advantages; in adsorption processes, make hydrogels superior in comparison to other conventional adsorbents. Due to flexible structure, high adsorption capacities, fast adsorption rates, and easy separation from adsorption medium, extensive research has been carried out on designing hydrogels and investigating their adsorption characteristics in the last few decades [1]. To this end, we have previously reported copolymer hydrogel consisting of methacrylic acid and hydroxylamine for the elimination of various pollutants such as organic dyes, herbicides, and heavy metal ions from contaminated water [5]. Luna *et al.* have reported chitosan based hydrogels containing cross-linked polymeric particles for the adsorptive removal of ionic dyes including rhodamine 6G, sunset yellow, indigo and carmine from aquatic medium [6]. Similarly, many other hydrogel systems have been prepared and investigated for the adsorptive removal of various metal ions and dyes which are known as highly toxic [7–12]. Except dyes and heavy metal ions, nitrophenols are another group of pollutants which contaminate water and have low adsorption affinities and therefore mostly reduced/degraded to get rid of their toxicity. The most commonly used reducing agent for the reduction of different nitrophenols is sodium borohydride ($NaBH_4$). However, the reduction of nitrophenols is hindered due to large kinetic barriers. Fortunately, the hindrance against the reduction of nitrophenols can be overcome with the aid of metal nanoparticles which act as catalyst and provide a new rout for the reduction reaction with low activation energy (E_a). In order to prevent the aggregation, metallic nanoparticles can be fabricated in hydrogel networks where they are stabilized by three dimensionally woven hydrogel networks. The as-prepared hydrogel embedded with nanoparticles of metals can be employed as catalyst to reduce nitrophenols. For example, Farooqi and coworkers [13] have prepared hydrogel by copolymerizing N-isopropylacrylamide with acrylic acid and fabricated silver (Ag) nanoparticles in that hydrogel system and found that the hydrogel had not only acted as a template to prepare Ag nanoparticles but also prevented the aggregation of the *in situ* prepared Ag nanoparticles. The hydrogel fabricated with Ag nanoparticles was found to act as good catalyst to enhance the reduction rate of the 4-NP. Farooqi *et al.* [14] have also reported the preparation of nickel (Ni) and cobalt (Co) nanoparticles in anionic hydrogel for the catalytic applications. The fabrication of metal nanoparticles in hydrogels for catalytic applications is advantageous due to their effortless and quick separation from the reaction medium by a very simple method of filtration upon the completion of reaction and reusability for several cycles. For example, Ajmal *et al.* [15] have synthesized Co and Cu nanoparticles in hydrogel matrices bearing amidoxime groups and investigated their catalytic properties in the reduction of nitro compounds and reported that the catalysts were having potential to be reused for many consecutive cycles without any substantial loss in catalytic activities. Similarly, preparation of gold (Au) nanoparticles in graphene oxide based hydrogels and investigation of their catalytic properties has been carried out by Adhikari *et al.* [16]. The authors reported that these composite hydrogel catalysts were easily recoverable and reusable for several cycles without significant loss in potency. So the hydrogels have great potential to be used for wastewater treatment by acting as adsorbents and as catalysts if suitable nanocatalysts are fabricated in their networks. In addition, hydrogels containing large numbers of carboxyl group in their network can swell to large extent and also can sorb huge amounts of oppositely charged pollutants from water. Therefore, it is pertinent to prepare hydrogel system containing large amounts of carboxyl groups and explore their ability for wastewater treatment. In this context, an effort was made by Seven and Sahiner [17] where they prepared poly(acrylic acid) hydrogel by a rather difficult, time and energy consuming, two step method that includes synthesis of poly(acrylamide) hydrogel in first step and then modification of amide groups into carboxyl groups in second step. Due to rather difficult and non-economical synthetic routs, use of hydrogels consisting of homopolymers of acrylic

acids for wastewater treatment has been very limited. In the present work, we have reported a single step facile synthesis of poly(methacrylic acid) [p(MAAc)] bulk hydrogel and investigated its adsorption behavior towards MB and Rh 6G. The hydrogel was also used as reactor as well as stabilizer for the Ni nanoparticles. The potential of the as-prepared Ni nanoparticles containing p(MAAc)-Ni hydrogel composite to act as a reusable catalyst was also evaluated by employing it as a catalyst for the reduction of 4-NP.

Experimental

Materials

Methacrylic acid (MAAc, 99.5 %, Duksan) was used as building block of hydrogel, while N,N′-methylenebisacrylamide (MBA, 99 %, sigma Aldrich) was used as a cross-linker, N,N,N′,N′-tetramethylethylene-1,2-diamine (TEMED, 98 %, Merck) was employed as accelerator and ammonium persulphate (APS, 98 %, Duksan) was utilized as an initiator. As a source of metal ions, we used Nickel (II) chloride hexahydrate ($NiCl_2 \cdot 6H_2O$, 99 %, Daejung). Sodium borohydride ($NaBH_4$, 98 %, Merck) was used as reducing agent for reduction reactions. Sodium hydroxide (NaOH, 99 %, sigma Aldrich) was utilized for neutralization of hydrogel. 4-Nitrophenol (4-NP, 99 %, Aldrich) was used as reactant in catalytic reduction reaction. Rhodamine 6G (Rh 6G) and Methylene blue (MB) were used as adsorbates. Distilled water was used during all the experimental work.

Synthesis of p(MAAc) polymer gel

P(MAAc) hydrogel was synthesized by free radical polymerization method. Total numbers of moles of MAAc were kept as 0.03. A 0.5 mol % (w.r.t MAAc) of APS and 1 mol % of MBA were used as initiator and cross-linker, respectively. As an accelerator, 200 µl of TEMED was used. Firstly in a glass vial, 0.046 g of MBA was dissolved in 1 ml of distilled water. Aqueous solution of MAAc was prepared by mixing its 2.55 ml in 2 ml distilled water. Solutions of both the monomer and cross-linker were mixed together in a glass vial. Then, 0.034 g of APS was added in 1 ml of distilled water and stirred to prepare its homogeneous solution and added in reaction mixture already containing monomer and cross-linker. After this, the reaction mixture was added with 200 µl TEMED as accelerator and homogenized by vigorous shaking. The homogenized reaction mixture was then filled in plastic straws and allowed to react at room temperature for 24 h. After 24 h, the prepared hydrogel was taken out from plastic straws and divided into small pieces. For cleansing, small pieces of hydrogels were placed in excess amount of distilled water. The hydrogel was kept in distilled water for 5 days and in this duration water was regularly changed 3 times in every 24 h to eliminate the impurities (such as unreacted species and foreign impurities). After washing, hydrogel was taken out from water, dried at 60 °C in oven. The dried hydrogel was stored in air tight containers for further use and characterization.

Synthesis of Ni nanoparticles in p(MAAc) hydrogel

To synthesize Ni nanoparticles in p(MMAc) hydrogel, firstly p(MAAc) hydrogel was treated with NaOH in aqueous medium for deprotonation. After deprotonation, hydrogel was cleansed by washing with distilled water thrice and dried in oven. For Ni (II) ion loading, 0.1 g of dried p(MAAc) hydrogel was added in 50 ml aqueous solution of Ni (II) having concentration of 500 ppm and stirred at 250 rpm for 2 h. In order to remove the loosely bound metal ions from the hydrogel matrices, the Ni (II) ions loaded hydrogel was washed with plenty of distilled water. After that the Ni (II) ions loaded hydrogel was dried in oven at 60 °C. Then 0.05 g of Ni (II) loaded hydrogel was treated with $NaBH_4$ in aqueous medium. A 50 ml aqueous solution of 0.1 M $NaBH_4$

was used. In this way metal ions were reduced and nanoparticles were formed in the networks of hydrogel. The prepared composite was filtered by using plankton cloth filter paper. The filtered composite was washed with distilled water and applied as catalyst. For characterization, the composite was dried in oven.

Catalytic activity

The performance of p(MAAc)-Ni composites as a catalyst was examined for reduction of 4-NP. $NaBH_4$ was added in the reaction medium as reducing agent. In a catalytic trial, 0.05 g p(MAAc)-Ni composite and 0.19 g of $NaBH_4$ was added to a 50 ml of 0.001 M aqueous solution of 4-NP. This reduction reaction was carried out in such an atmosphere where the temperature was kept constant throughout the reaction time. A 300 µl of reaction mixture was separated from the reaction medium at different intervals of time, diluted 15 times with distilled water and Ultra violet-Visible (UV-Vis) spectra of samples were subsequently recorded by UV-Vis spectrophotometer. The progress of reaction was observed from the decrease in absorbance peak at 400 nm with the passage of time. Influence of temperature on catalytic process was examined by conducting the reaction at various temperatures in the temperature window of 30–60 °C while keeping the amounts of catalyst and reactant constant. Different amounts of catalyst were also used to observe the effect of amount of catalyst.

Adsorption study

The adsorption study was carried out by using the prepared p(MMAc) hydrogel for the adsorptive removal of two industrial dyes; MB and Rh 6G from aqueous medium. Effects of adsorbent dose and that of initial concentration of adsorbate solution were studied. The amounts of dyes adsorbed on p(MAAc) were measured in terms of decrease in absorbance of dyes at their maximum absorption wavelengths (664 nm for MB, 530 nm for Rh 6G). To analyze the influence of amount of hydrogel on the percent removal of dyes from water, various amounts of p(MAAc) hydrogel; 0.05, 0.1, 0.15, and 0.2 g were added in 100 ml solution of each of MB (150 ppm) and Rh 6G (48 ppm) in separate containers. The adsorption medium was stirred at 250 rpm and the hydrogel was allowed to adsorb dye from the medium. During the process of adsorption, certain amount of sample was withdrawn from adsorption medium and amount of adsorbed dye was calculated in terms of measurements of absorbance of the sample by UV-Vis spectrophotometer. For isotherm studies, experiments were carried out by taking 100 ml solution of each dye having different initial concentrations (50, 100, 200, 400, 600, 800, and 1000 ppm for MB and 24, 48, 96, 120, 144, and 192 ppm for Rh 6G) in separate containers and 0.05 g of p(MAAc) hydrogel was put together as adsorbent in each container.

Results and discussions

Synthesis of P(MAAc) hydrogel and (MAAc)-Ni composite

P(MAAc) hydrogel was prepared by simultaneous polymerization and cross-linking of prepared polymer chains using free radical polymerization technique. In this process, the initiator i.e. APS produces persulphate ions which are then changed into sulphate ion radicals. These sulphate ion radicals start the polymerization process. The free radicals of initiator react with monomers and cross-linkers to produce new free radicals possessing highly reactive nature. These reactive species react with each other and in this way polymer chains propagate. The cross-linker links the polymer chains with each other through chemical bonding and as a result the polymeric structure extends in three dimensions. The obtained three dimensional network of p(MMAc) hydrogel was applied as a medium to prepare Ni nanoparticles *in situ*. A pathway for the

preparation of Ni nanoparticles in p(MMAc) hydrogel along with physical appearance of reaction medium is shown in Fig. 1. P(MAAc) hydrogel contain numerous carboxylic groups (–COOH) which were converted to negatively charged carboxyl ($–COO^-$) groups by deprotonation. The deprotonation was carried out by treating p(MAAc) hydrogel with NaOH. The digital camera image (1) in Fig. 1 represents that deprotonated p(MAAc) hydrogel was off-white colored. The deprotonated p(MAAc) hydrogel was immersed in Ni (II) ions solution and Ni (II) ions were laden in hydrogels due to force of attraction between oppositly charged Ni (II) ions and $–COO^-$ groups. The loading of Ni (II) ions was observed via color change of hydrogel from off-white to light green as depicted by digital camera image (2) in Fig. 1. When this metal ion loaded hydrogel was treated with $NaBH_4$ then it was converted into black color as shown in digital camera image 3 in Fig. 1 which was the indication of formation of Ni nanoparticles [18, 19].

Characterization

The swelling behavior of p(MAAc) hydrogel was studied in terms of measuring the capacity of p(MAAc) hydrogel to absorb water. For this purpose, a weighed quantity of dried p(MAAc) hydrogel was added in distilled water and was allowed to swell by absorbing water. The amount of water entrapped by p(MAAc) hydrogel was determined by measuring weight of hydrated hydrogel at various intervals of time till the saturation point. The percent swelling was calculated by following formula

$$S\,\% = (M_t - M_d)/M_d \times 100$$

where, M_d is mass of the hydrogel in dried form which was added in water to swell and M_t is weight of hydrogel at various intervals of time during swelling. The swelling experiments were carried out in triplicate and the average values of percent swelling are presented here.

The percent swelling of p(MAAc) hydrogel with time is represented in Fig. 2a which depicts that maximum swelling was attained in 24 h. However, initially swelling rate was very high but with the passage of time swelling rate was decreased. The decrease in swelling rate after certain time might be to the reason that the empty space in hydrogel network at easiest approach were filled with water quickly and after that water molecules take comparatively larger time to diffuse through the hydrogel network. The swelling of hydrogel can also be seen from the physical states as shown by digital camera images (1) and (2) of dried and water

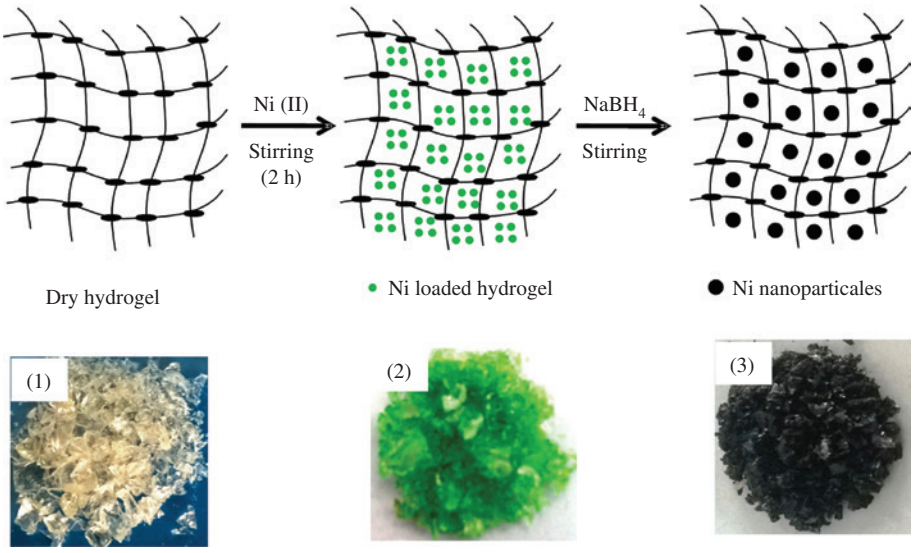

Fig. 1: Schematic representation for the synthesis of p(MAAc)-Ni composite and digital camera images of **(1)** p(MAAc) hydrogel and **(2)** p(MAAc) hydrogel loaded with Ni (II) ions, and **(3)** p(MAAc) hydrogel loaded with Ni nanoparticles.

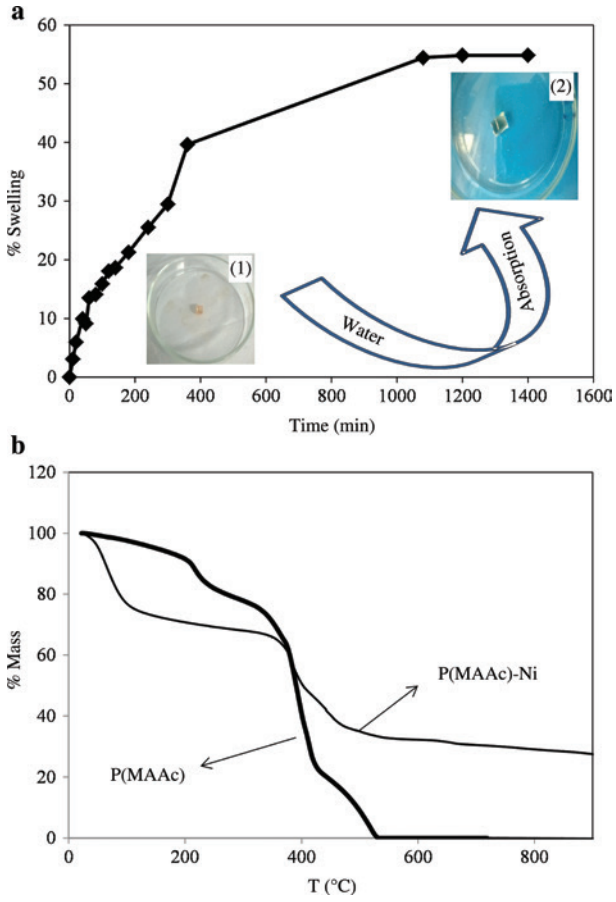

Fig. 2: (a) Plot of % swelling vs. time for swelling of p(MAAc) hydrogel in distilled water **(1)** digital camera image of hydrogel before swelling and **(2)** after swelling. (b) TGA thermograms of p(MAAc) hydrogel and p(MAAc)-Ni hydrogel composite.

swollen p(MAAc) hydrogel, respectively, in Fig. 2a. The dried piece of hydrogel seems to be very hard but after absorbing water it becomes soft and transparent glassy material. Thermal characteristics of the prepared hydrogel were explored with the help of TGA. Figure 2b shows the thermograms of pure and composite hydrogel which depict that thermal degradation of pure hydrogel was occurred in four steps. In first step, a 10 % decrease in weight was occurred with the increase in temperature to 210 °C which may be due to elimination of entrapped water molecules. The second step of thermal degradation was observed in the temperature window of 210–321 °C with another 15 % weight loss. This observation may be associated to breakdown of weakly crosslinked outer surface of hydrogels. In third and fourth steps, very rapid weight loss of 54 % and 20 % was observed in the temperature window of 321–435 °C and 435–530 °C, respectively. In this way the total decrease of weight was reached to 99 % upon raising the temperature to 530 °C. The rapid degradation in third and fourth steps can be due to the fact that thermal energy in the corresponding temperature windows was high enough to break the hydrogel network. For p(MAAc)-Ni composite three step thermal degradation was observed with 25 % loss of weight in the temperature window of 35–105 °C, 8 % weight loss in the temperature range of 105–365 °C, and another 35 % in the temperature window of 365–540 °C. This three step pattern of thermal degradation may be due to a strong crosslinking in the internal region and weak crosslinking in the external region of hydrogel networks. The overall lower weight loss indicates the presence of metallic material in the hydrogel which is off course Ni. The higher thermal stability of composite hydrogel can be achieved because of the presence of Ni nanoparticles in the networks of hydrogel. Actually, Ni nanoparticles develop a coordination interaction with functional groups of polymer present in polymeric chains of hydrogel because of possessing charge density on the Ni nanoparticle's surfaces [20]. Such an interaction increases the mechanical strength of hydrogel system and enhances its thermal stability.

Ni nanoparticles fabricated in p(MAAc) hydrogel were seen by TEM. Figure 3a represents TEM image of the Ni nanoparticles embedded in p(MAAc) hydrogel networks. The absence of any aggregates revealed the potential of p(MAAc) hydrogel to prevent the coagulation of Ni nanoparticles. From the TEM image, the estimated size of Ni nanoparticles is in the range of 6–10 nm. For phase identification of the prepared hydrogel and its corresponding composite, XRD patterns were recorded. Figure 3b shows XRD patterns of p(MAAc) and p(MAAc)-Ni. A broad peak in XRD pattern of p(MAAc) hydrogel networks around 2θ value of 25 was obtained due to amorphous polymeric structure. The Ni nanoparticles possess crystalline nature and they exhibit sharp peaks in XRD pattern which were not observed in case p(MAAc)-Ni composite but it is obvious because the sharp peaks are suppressed due to abundance of polymeric hydrogel networks which act as continuous phase in p(MAAc)-Ni composite [21]. However, the presence of Ni nanoparticles was proven by TEM. The elemental analysis was done by using EDS. The EDS spectrum of p(MAAc)-Ni composite hydrogel is shown in Fig. 4a. The major elements present in p(MAAc)-Ni composite hydrogel indicated by EDS were carbon (C), oxygen (O), sodium (Na), and Ni with their corresponding percentage of 41.33 %, 37.76 %, 12 %, and 8.51 %, respectively. The abundant amount of C and O were observed due to their large amount in p(MAAc) which was continuous phase of p(MAAc)-Ni composite while Na might be entrapped in hydrogel or Ni nanoparticle's cavities during the *in situ* reduction of Ni (II) in hydrogel matrices. The appearance of a noticeable amount of Ni in EDS spectrum proved the fabrication Ni nanoparticles in p(MAAc) hydrogel. FT-IR spectra of p(MAAc) hydrogel and p(MAAc)-Ni hydrogel composite are shown in Fig. 4b. The carbonyl (–C=O) of carboxyl group showed its stretching at 1204 cm^{-1}. The absorption peaks at 1390 and 1470 cm^{-1} were due to bending of C–H of methyl group while a peak at 1700 cm^{-1} was corresponding to –C=O stretch. The two absorption bands were observed at 2970 and 2930 cm^{-1} for asymmetric and symmetric stretching of C–H bond, respectively.

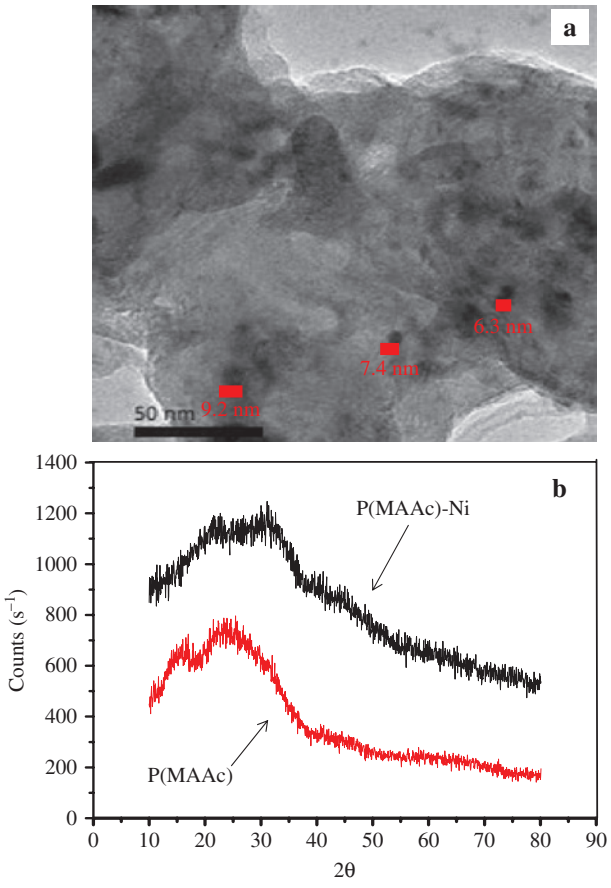

Fig. 3: (a) TEM image of the Ni nanoparticles fabricated in p(MAAc) hydrogel. (b) XRD patterns of p(MAAc) and p(MAAc)-Ni.

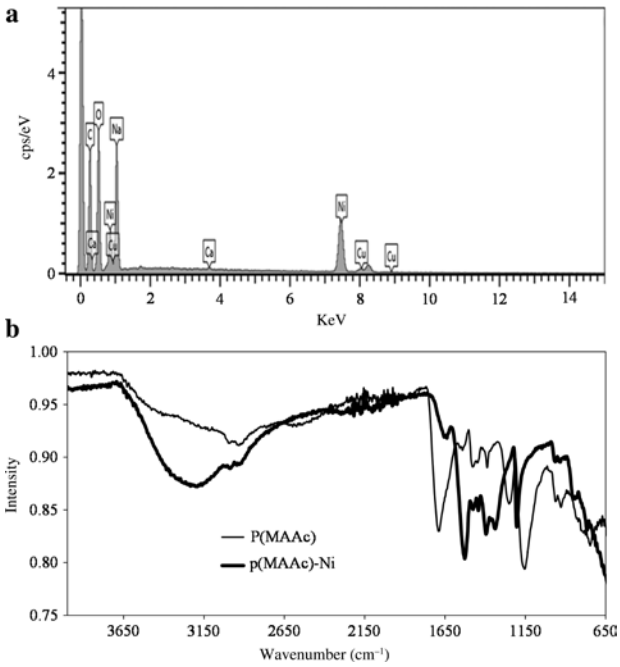

Fig. 4: (a) EDX spectrum of p(MAAc)-Ni hydrogel composite. (b) FT-IR spectra of p(MAAc) hydrogel and p(MAAc)-Ni hydrogel composite.

FT-IR spectrum of p(MAAc) hydrogel showed no absorption band in the region of 1640–1680 cm^{-1} which indicated the absence of C=C double bond in the structure of p(MAAc) hydrogel and confirmed the polymerization. A broad band at 3300 cm^{-1} in FT-IR spectrum corresponds to O–H stretching was showing hydrogen bonding of water molecules with –C=O group present inside the hydrogel network. After the fabrication of Ni nanoparticles, the FT-IR spectrum of hydrogel was similar to that of bare hydrogel in all respects except that the intensity of the absorption band of –C=O of carboxyl group was decreased while the intensity of absorption band of C–H of the methyl group was increased. This slight change in FT-IR spectra can be observed due to coordination interaction between Ni nanoparticles and carboxyl groups [20].

Adsorption study

The prepared p(MAAc) hydrogel was utilized as adsorbent for the adsorptive removal of MB and Rh 6G from aqueous medium. The presence of these dyes in water causes toxicity. These dyes cause severe effects on human health like carcinogenic, shock and increase in heartbeat [22, 23]. So, their removal from water is essential. In a systematic adsorption study, first of all effect of adsorbent dose was analyzed. For this purpose, 150 ppm solution of MB was prepared and its 100 ml was taken in four separate containers. Each container was added with various amounts of p(MAAc) hydrogel; 0.05, 0.10, 0.15, and 0.20 g as adsorbent. The percent (%) removal of MB and Rh6 G dyes from their aqueous solutions with the passage of time is represented in Fig. 5a and b, respectively. Figure shows that with the increase in amount of adsorbate from 0.05 to 0.20 g the percentage of dyes removed from water was increased from 96 to 98 % for MB and 87–91 % in the case of Rh 6G. It was observed that the rate of adsorption was also increased with increase in adsorbent dose which was indicated from the movement of plots of % removal of dye against time towards horizontal axis. Such an increase in adsorption rate can occur because of increase in adsorption sites within adsorption medium. In the presence of greater adsorption active sites, greater numbers of adsorbate molecules are attached on the surface in unit time and hence the adsorption rate is increased. The Fig. 5a and b also represent that there was anomalous behavior in % age removal of both the dyes as a function time. This anomalous behavior can

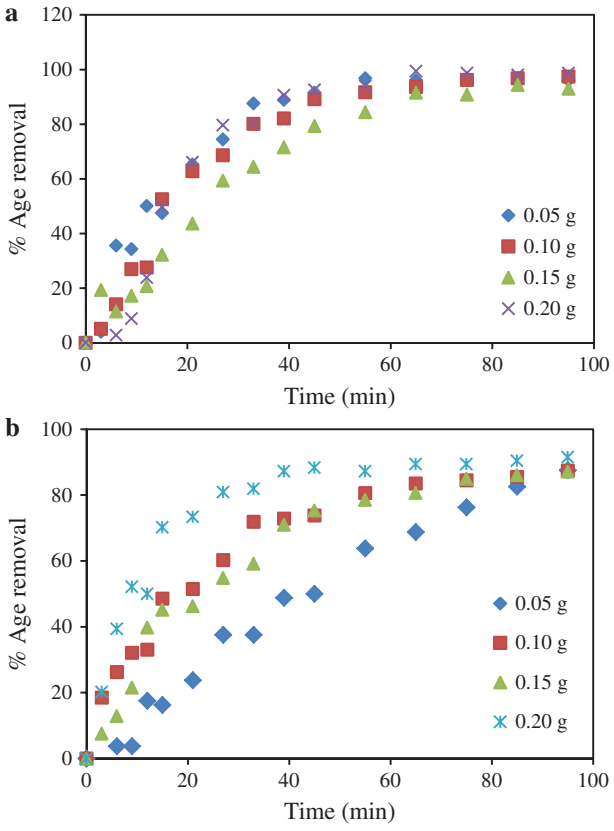

Fig. 5: Graphs of % removal of dyes *vs*. time with various amounts of p(MAAc) hydrogel. (a) MB [100 ml, 150 ppm] and (b) Rh 6G [100 ml, 40 ppm].

be observed due to similarity in the charges on adsorbate and equivalency in adsorption sites on adsorbent. The adsorption of both the dyes was observed on same adsorbent so the adsorption sites on adsorbent for both dyes were equivalent. In addition, both the dyes possess unit positive charge in aqueous medium which becomes responsible for their anomalous adsorption behavior.

The concentration of adsorbate solution is another factor that also influences the process of adsorption. So, in this work we also evaluated the effect of change in initial concentration of adsorbate solution. In the case of MB, aqueous solutions of initial concentrations of 50, 100, 200, 400, 600, 800, and 1000 ppm were studied. While for Rh 6G, the different initial concentrations of 24, 48, 96, 144, and 192 ppm of solution were used. For 100 ml solution of each concentration, 0.05 g of dried p(MAAc) hydrogel was used as adsorbent.

Figure 6a and b represents the amounts of MB and Rh 6G, respectively, adsorbed per gram of dried p(MAAc) hydrogel at different intervals of time. The quantity of MB adsorbed was increased from 80 to 685 mg/g corresponding to increase in concentration of MB from 50 to 1000 ppm. In the case of Rh 6G, the amount of dye adsorbed increased from 260 to 1571 mg/g with increasing the concentration from 24 to 192 ppm. The increase in adsorbed amount with the increase in concentration of adsorbate solution shows that with lower concentration of adsorbate solution the adsorption sites of adsorbent were not occupied to saturation level. However, with increase in concentration of adsorbate, the active adsorption sites were gradually occupied and hence an increase in adsorption capacity was observed. Although, both the MB and Rh 6G are cationic dyes but they differ in chemical composition, chemical structure, molecular weight and solubility in water. Therefore, different amounts of these two dyes were found to be adsorbed on the unit mass of same adsorbent. The greater adsorption capacity of adsorbent for Rh G as compared to MB can be explained on the basis of molecular weight and solubility in water. Molecular weight of Rh 6 G is 479.02 g/mol while that of MB is 319.85 g/mol. On the other hand, the solubility of Rh 6G in water at room temperature is 20 g/L while

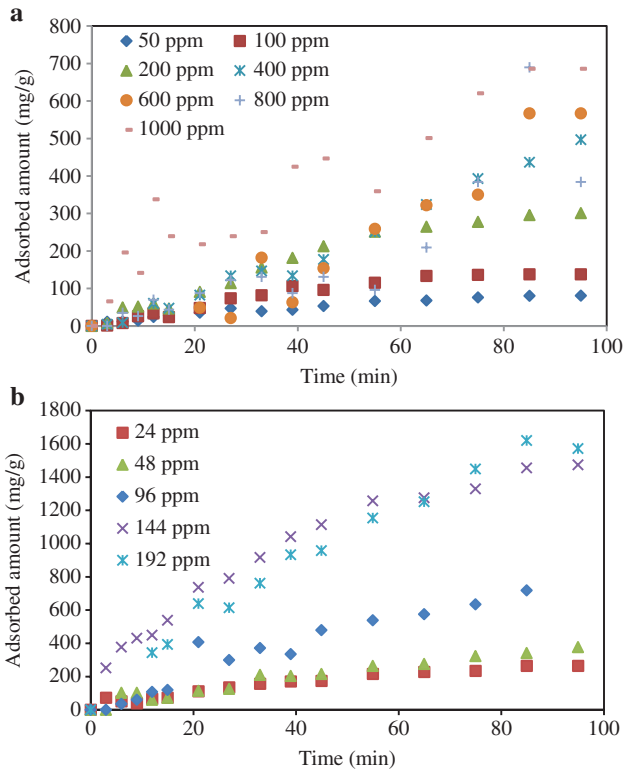

Fig. 6: Plots of amounts of (a) MB and (b) Rh 6G adsorbed on p(MAAc) from their aqueous solutions of different concentrations. [Reaction conditions; p(MAAc) = 0.05 g, MB or Rh 6G solution = 100 ml, 100 rpm, 30 °C].

that of MB is 43.6 g/L. Due to lower solubility, Rh 6G has comparatively greater affinity to detach from water and attach on the active adsorption sites. Another deriving force for the adsorption is the charge on adsorbate and adsorbent. Both the MB and Rh 6G have unit positive charge while the adsorption sites for both the dyes are equivalent. The mass (molecular weight) of unit charge of Rh 6G is much larger as compared to that of MB. Due to the greater mass of unit charge of Rh 6G, the adsorption capacity of p(MAAc) hydrogel was observed to be greater for Rh 6G as compared to that for MB. Similar results of adsorption of MB and Rh 6G on the acrylic acid based adsorbents have been reported by Shukla and Madras [24].

Adsorption isotherms

It is important to understand the mechanism of accumulation which is usually studied by the application of various adsorption isotherms. Therefore, the data obtained from the adsorptive removal of MB and Rh 6G was treated with well-known Langmuir, Freundlich, and Temkin adsorption isotherms. Mathematical expressions of the applied isotherms are given below by expressions (1–3).

$$\text{Langmuir} \quad \frac{C_e}{q_e} = \frac{C_e}{q_m} + \frac{1}{q_m K_L} \tag{1}$$

$$\text{Freundlich} \quad \log q_e = \frac{1}{n} \log C_e + \log K_F \tag{2}$$

$$\text{Temkin} \quad q_e = B \ln C_e + B \ln K_T \tag{3}$$

where, C_e is concentration of aqueous solution of dye in ppm at equilibrium condition of adsorption process, q_e represents the quantity of dye in mg accumulated on per gram of hydrogel at equilibrium condition,

and q_m is highest quantity of dye accumulated on per gram of hydrogel. The parameter K_L is known as equilibrium Langmuir constant and it explains the ability of an adsorbent to be in equilibrium with adsorbate. The parameter K_F is known as Freundlich adsorption constant and corresponds to the adsorption capacity while the constant n corresponds to adsorption intensity and also known as heterogeneity parameter. The term B is a constant corresponding to heat of adsorption and K_T represents the equilibrium binding constant and corresponds to the maximum value of binding energy. The value of B depends upon temperature according to following equation (4)

$$B = \frac{RT}{b_T} \tag{4}$$

where, b_T, R, and T are Temkin constant, general gas constant and temperature in Kelvin, respectively. The relation between C_e and q_e is shown in Fig. 7a. Langmuir adsorption model assumes that all the adsorption sites are equivalent to each other and further assumes that once an active site is occupied by an adsorbate molecule no further molecule can adsorb at that site and hence monolayer adsorption can occur. Figure 7b depicts the graphical expression of Langmuir adsorption isotherm. The values of determination of coefficients (R^2), q_m and K_L for both the MB and Rh 6G are given in Table 1. For MB, the R^2 value was very close to 1 and q_m value was in close resemblance with experimental value. These values of R^2 and q_m, suggested that attachment of MB on hydrogel was most probably followed by Langmuir model and it was accumulated on the surface of p(MMAc) hydrogel in the form of a monolayer. However, the values of constants for Rh 6G suggested that adsorption of Rh 6G was not occurred according to Langmuir adsorption model. The influence of surface roughness and probability of accumulation of adsorbate in the form of multilayers on the surface of adsorbent is covered by Freundlich adsorption model. As shown in Fig. 7c, graphical forms of Freundlich adsorption isotherm for both the MB and Rh 6G were obtained by plotting the graph between log q_e and log C_e.

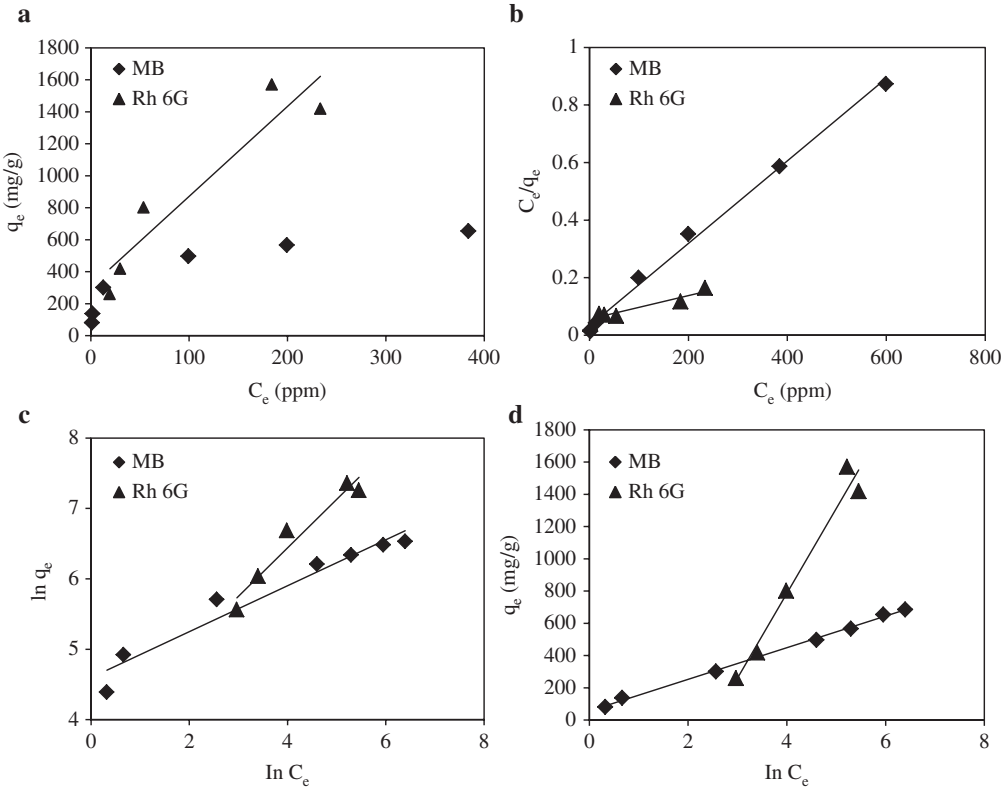

Fig. 7: Graphs of (a) C_e vs. q_e. (b) Langmuir adsorption isotherm. (c) Freundlich adsorption isotherm. (d) Temkin adsorption isotherm for the adsorption of MB and Rh 6G on p(MAAc) hydrogel.

The values of constants n and K_F were calculated from slope and intercept of Freundlich adsorption isotherm and are shown in Table 1. Although, the value of n and R^2 represented that the adsorption was following the Freundlich adsorption model however, the value of K_F disagreed to experimental data for both the dyes. There is another adsorption model according to which heat changes during the adsorption process as well as the possible mutual interaction of adsorbate and adsorbent may also affect the adsorption rate and capacity. This is known as Temkin adsorption isotherm. The ln C_e was plotted against q_e to obtain Temkin isotherm as shown in Fig. 7d. The slope and intercept of the graph were used to calculate the values of B and K_T, respectively. Table 1 represents the values of these constants. The value of R^2 obtained for Rh 6G was 0.992 which was more close to one than the value obtained from other isotherms which was the indication that adsorption Rh 6G was most probably followed by Temkin adsorption model.

Catalytic study

The catalytic activity of p(MAAc)-Ni composite was studied by using it as a catalyst to speed up the reduction of 4-NP in water in the presence of a reducing agent, $NaBH_4$. In aqueous medium, the absorption spectrum 4-NP gives maximum absorption at 317 nm [25]. When $NaBH_4$ is added in aqueous solution of 4-NP then the absorbance peak appears at 400 nm with a red shift due to phenolate ion formation. Since 4-NP is UV-Vis active, so its reduction was observed by measuring its absorbance with UV-Vis spectrophotometer at 400 nm during the course of reaction. The absorbance at 400 nm was deceased while concomitantly a new absorption peak of 4-AP was appeared at 300 nm as depicted by Fig. 8a.

The amount of $NaBH_4$ was kept hundred times greater than amount of 4-NP so the reaction was supposed to be pseudo 1st order [26, 27]. So rate of reaction was calculated by applying pseudo 1st order kinetics whose mathematical expression is given below by equation 5.

$$\ln\frac{C_t}{C_o} = -k_{\text{app}} \cdot t \tag{5}$$

Here, C_o and C_t indicate concentrations of 4-NP at zero time and time t during the reaction, and k_{app}; equal to product of molar concentration of $NaBH_4$ and absolute rate constant, is apparent rate constant. According to Beer's law, concentration of a substance is directly proportional to the intensity of its absorption peak. Therefore, for 4-NP the value of C_t/C_o was calculated from the absorbance ratios of 4-NP taken at time t (A_t) and at time 0 min (A_o). The reduction of 4-NP was performed in the temperature window of 30–60 °C by regular variation of 10 °C. The amount of catalyst, concentration of 4-NP solution and volume of 4-NP was kept same for every temperature. Speed of reaction was measured in terms k_{app} which was calculated using the slopes of straight line graphs obtained for pseudo 1st order kinetics and shown in Fig. 8b. The values of the slopes were enhanced by raising the temperature and hence an increase in reduction rate was also observed. In

Table 1: Kinetic parameters calculated from three adsorption isotherms for the adsorption of Rh 6G and MB on p(MAAc) hydrogel.

	MB			**Rh6 G**		
Langmuir isotherms constants	R^2	K_L (L/g)	q_m (mg/g)	R^2	K_L (L/g)	q_m (mg/g)
	0.995	0.044	714.28	0.912	0.007	2500
Freundlich isotherm constants	R^2	K_F (L/g)	n	R^2	K_F (L/g)	n
	0.947	99.18	3.070	0.944	40.00	1.45
Temkin isotherm constants	R^2	K_T (L/g)	B	R^2	K_T (L/g)	B
	0.969	1.5×10^{-6}	98.045	0.997	1.11	525.6

Reaction conditions; p(MAAc) = 0.05 g, solution of dye = 100 ml, concentration of dye = (Rh 6G 24 – 192 ppm, MB 50 – 800 ppm) room temperature, 100 rpm. R^2, determination of coefficients; K_L, equilibrium Langmuir constant; K_F, Freundlich adsorption constant; B, heat of adsorption constant; K_T, equilibrium binding constant; q_m, maximum adsorption capacity; n, heterogeneity parameter.

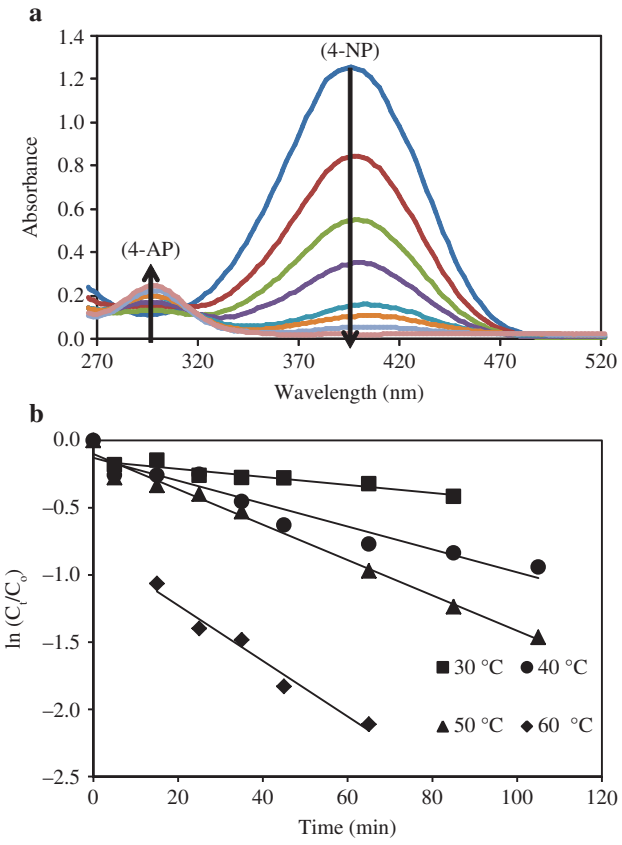

Fig. 8: (a) UV-Visible Spectra for the reduction of 4-NP catalyzed by p(MAAc)-Ni composite at 30 °C. (b) Plots of $\ln(C_t/C_o)$ against time for the reduction of 4-NP at different temperatures. Reaction conditions: 0.01 M 4-NP = 50 ml, $NaBH_4$ = 0.19 g, p(MAc)-Ni = 0.1 g, 250 rpm, 30 °C.

fact, by raising the temperature, we actually raise the average kinetic energy of molecules and the molecules with increased kinetic energy diffuse towards the surface of catalyst with higher diffusion rate which finally speeds up the rate of 4-NP reduction.

The data obtained by this catalytic reduction at different temperatures was useful for measuring activation parameters. Arrhenius equation was used for calculation of activation energy (E_a). Arrhenius equation is given as follows

$$\ln k_{app} = -\frac{E_a}{RT} + \ln A \tag{6}$$

According to above mathematical relation 6, a graph was plotted between $\ln k_{app}$ and $1/T$ as shown in Fig. 9a. The slope of this graph gives the E_a which was found to be 52 KJ/mol. In addition to measurement of E_a, thermodynamic parameters were also calculated. Eyring Equation (7) was used to calculate the activation entropy change ($\Delta S^{\#}$) and activation enthalpy change ($\Delta H^{\#}$).

$$\ln\left(\frac{k_{app}}{T}\right) = -\frac{\Delta H^{\#}}{RT} + \left[\ln\left(\frac{k_B}{h}\right) + \left(\frac{\Delta S^{\#}}{R}\right)\right] \tag{7}$$

Where, k_{app} is apparent rate constant, k_B is Boltzmann constant, h is Planks constant, R is general gas constant, T is temperature in K, while $\Delta S^{\#}$ and $\Delta H^{\#}$ are representing the activation entropy and activation enthalpy change, respectively. A graph of $1/T$ against $\ln k_{app}/T$ was plotted as shown in Fig. 9b.

The slope of this graph was equal to $\Delta H^{\#}/R$ and value of $\Delta H^{\#}$ was calculated from this slope and was found to be −49.435 kJ/mol. The negative value of $\Delta H^{\#}$ represents that activated complex was formed in exothermic

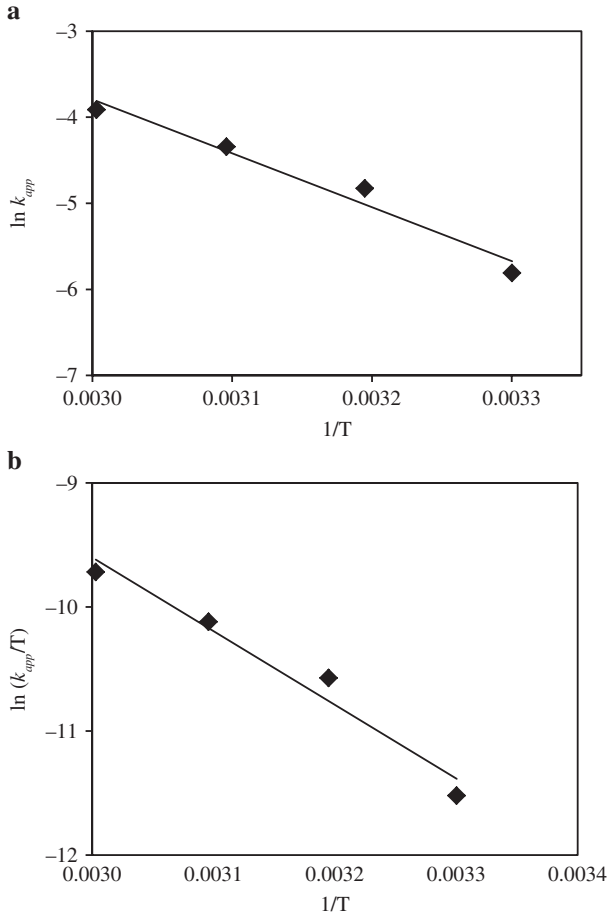

Fig. 9: Plot of (a) ln k_{app} vs. 1/T and (b) k_{app}/T vs. 1/T for the reduction of 4-NP catalyzed by p(MAAc)-Ni. Reaction conditions; 0.01 M 4-NP = 50 mL, $NaBH_4$ = 0.19 g, catalyst = 0.002 g, 250 rpm.

process during the reduction of 4-NP. The value of $\Delta S^{\#}$ was calculated by using intercept of the plot ln (k_{app}/T) against $1/T$ which was equal to –129 J $mol^{-1}K^{-1}$. The value of $\Delta S^{\#}$ with negative sign reveals that as compared to reactants the activated complex was in more ordered form and its formation was occurred by association mechanism.

To calculate Gibbs free energy change ($\Delta G^{\#}$), mathematical equation is given below

$$\Delta G^{\#} = \Delta H^{\#} - T\Delta S^{\#} \tag{8}$$

In this equation T is temperature of the reaction medium in Kelvin. The values of $\Delta G^{\#}$ for 4-NP reduction were found to be 39.15, 40.39, 41.68, and 42.99 KJ mol^{-1} at 30, 40, 50, and 60 °C, respectively. These values of $\Delta G^{\#}$ are positive and therefore represent that the reduction process of 4-NP was non-spontaneous and required an external aid which was offered by the catalyst in the reaction mixture. The thermodynamic parameters indicate that the reaction feasible in the presence of catalyst. If a reaction is catalyzed by some catalyst then its rate is also influenced by the amount of catalyst so the investigation of the effect of amount of catalyst is also pertinent. 4-NP reduction was performed in the presence of different amounts of p(MAAc)-Ni composite in the reaction medium as catalyst. Figure 10a represents the variations in reduction rate of 4-NP corresponding to variations in amount of catalyst. The results showed that an increase of catalyst dose results in an increase in reaction rate which is evident by increase in slopes of corresponding plots in Fig. 10a. Such an increase in rate of reaction is associated to increase in the numbers of catalytic sites which in turn increases the rate of adsorption and desorption on and from the surface of catalyst which eventually results in an enhancement of

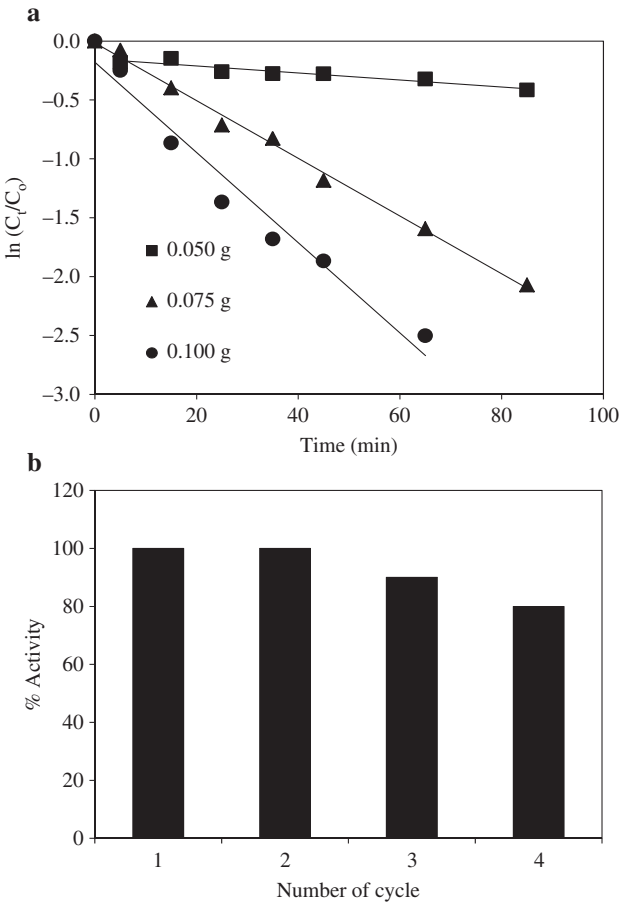

Figure 10: (a) Plots of $\ln(C_t/C_o)$ against time for the reduction of 4-NP catalyzed by different amounts of p(MAAc)-Ni. (b) Change in % activity of p(MAAc)-Ni catalyst in four consecutive cycles for the reduction of 4-NP. Reaction conditions; 0.01 M 4-NP = 50 ml, $NaBH_4$ = 0.19 g, 250 rpm, 30 °C.

rate of the reaction. From technical and economical view point, easy removal of the catalysts from the reaction medium and its reuse is very important. Therefore, reusability of p(MAAc)-Ni catalyst we also studied. The catalyst was removed from the reaction mixture by a very fast and easy process of filtration. The filtration was carried out with plankton cloth filter paper. The filtered catalyst was then cleaned by washing with distilled water. The cleansed catalyst was reused in the next cycle of same reaction. The filtered catalyst was washed with distilled water and used again for the reduction of 4-NP under same reaction conditions. This process was repeated for four consecutive cycles and change in catalytic activity was determined by measuring the rate constant for every cycle. The change in % activity of catalyst with number of cycles is shown in Fig. 10b.

It was observed that activity of the catalyst was gradually decreased from 100 to 80 % as we reached from 1st to 4th cycle. This loss in activity of p(MAAc)-Ni catalysts may occur due to leaching of some metal nanoparticles during washing process or due to the formation of oxide layer on the surface of Ni nanoparticles [18]. The oxidation may occur because of oxidizing nature of Ni nanoparticles.

Conclusions

Synthesis of p(MAAc) hydrogel by free radical polymerization and fabrication of Ni nanoparticles in p(MAAc) hydrogel networks by *in situ* chemical reduction was accomplished. The high adsorption capacity of p(MAAc) hydrogel for MB (685 mg/g) and Rh 6G (1571 mg/g) revealed that P(MAAc) hydrogel has great potential to be

used as adsorbent for the adsorptive removal of Rh 6G and MB from water. Temkin, Langmuir and Freundlich adsorption isotherms were applied on the adsorption data and it was found that adsorption data of MB was best fitted with Langmuir isotherm and that of Rh 6G with Temkin adsorption isotherm. Additionally, p(MAAc)-Ni was found to act as a catalyst for the reduction of 4-NP. Reduction of 4-NP was found to be a function of both temperature and catalyst dose and rate of reduction of 4-NP was increased by increasing any of these parameters. Furthermore, the catalyst was easily recoverable by a simple and fast process of filtration and only 20 % loss in catalytic activity in fourth consecutive cycle was observed. Overall, this work reveals that prepared p(MAAc) hydrogel was having great potential to act as adsorbent for cationic pollutants and as a template for the preparation of metallic nanoparticles such as Ni, while the resultant p(MAAc)-Ni composite act as easily recoverable and reusable catalyst with promising catalytic activity.

References

[1] G. Jing, L. Wang, H. Yu, W. A. Amer, L. Zhang. *Colloids Surf. A Physicochem. Eng. Asp.* **416**, 86 (2013).
[2] D. Mohan, A. Sarswat, Y. S. Ok, C. U. Pittman. *Bioresour. Technol.* **160**, 191 (2014).
[3] R. Begum, R. Rehan, Z. H. Farooqi, Z. Butt, S. Ashraf. *J. Nanopart. Res.* **18**, 231 (2016).
[4] M. Khan, I. M. Lo. *Water Res.* **106**, 259 (2016).
[5] M. Ajmal, M. Siddiq, N. Aktas, N. Sahiner. *RSC Adv.* **5**, 43873 (2015).
[6] M. S. de Luna, R. Castaldo, R. Altobelli, L. Gioiella, G. Filippone, G. Gentile, V. Ambrogi. *Carbohydr. Polym.* **177**, 347 (2017).
[7] R. Fang, W. He, H. Xue, W. Chen. *React. Funct. Polym.* **102**, 1 (2016).
[8] R. Xu, G. Zhou, Y. Tang, L. Chu, C. Liu, Z. Zeng, S. Luo. *Chem. Eng. J.* **275**, 179 (2015).
[9] W. Feng, W. Wenbo, Z. Yongfeng, W. Aiqin. *J. Rare Earths* **35**, 697 (2017).
[10] X. Wang, R. Sun, C. Wang. *Colloids Surf. A Physicochem. Eng. Asp.* **441**, 51 (2014).
[11] F. Bibi, M. Ajmal, F. Naseer, Z. Farooqi, M. Siddiq. *Int. J. Environ. Sci. Technol.* **15**, 863 (2018).
[12] F. Naseer, M. Ajmal, F. Bibi, Z. H. Farooqi, M. Siddiq. *Polym. Compos.* **39**, 3187 (2018).
[13] Z. H. Farooqi, S. R. Khan, T. Hussain, R. Begum, K. Ejaz, S. Majeed, M. Ajmal, F. Kanwal, M. Siddiq. *Korean J. Chem. Eng.* **31**, 1674 (2014).
[14] Z. H. Farooqi, S. Iqbal, S. R. Khan, F. Kanwal, R. Begum. *e-Polymers* **14**, 313 (2014).
[15] M. Ajmal, S. Demirci, M. Siddiq, N. Aktas, N. Sahiner. *New J. Chem.* **40**, 1485 (2016).
[16] B. Adhikari, A. Biswas, A. Banerjee. *ACS Appl. Mater. Inter.* **4**, 5472 (2012).
[17] F. Seven, N. Sahiner. *J. Appl. Polym. Sci.* **131**, 41106 (2014).
[18] M. Ajmal, M. Siddiq, H. Al-Lohedan, N. Sahiner. *RSC Adv.* **4**, 59562 (2014).
[19] M. Ajmal, S. Demirci, M. Siddiq, N. Aktas, N. Sahiner. *Colloids Surf. A Physicochem. Eng. Asp.* **486**, 29 (2015).
[20] H. H. Patterson, R. S. Gomez, H. Lu, R. L. Yson. *Catal. Today* **120**, 168 (2007).
[21] T. Altınçekiç, I. Boz, A. Basaran, B. Aktaş, S. Kazan. *J. Supercond. Nov. Magn.* **25**, 2771 (2012).
[22] M. Zendehdel, A. Barati, H. Alikhani, A. Hekmat. *J. Environ. Health Sci. Eng.* **7**, 431 (2010).
[23] S.-Y. Mak, D.-H. Chen. *Dyes Pigm.* **61**, 93 (2004).
[24] N. B. Shukla, G. Madras. *J. Appl. Polym. Sci.* **126**, 463 (2012).
[25] D. Rambabu, C. P. Pradeep, A. Dhir. *New J. Chem.* **39**, 8130 (2015).
[26] Y. Lu, J. Yuan, F. Polzer, M. Drechsler, J. Preussner. *ACS Nano* **4**, 7078 (2010).
[27] Y. Mei, Y. Lu, F. Polzer, M. Ballauff, M. Drechsler. *Chem. Mater.* **19**, 1062 (2007).